Residual Monte Carlo Transport in Time with Consistent Low-Order Acceleration for 1D Thermal Radiative Transfer

Simon R. Bolding and Jim E. Morel

Texas A&M University Nuclear Engineering Department,
sbolding@tamu.edu, morel@tamu.edu

INTRODUCTION

Accurate solutions to the thermal radiative transfer (TRT) equations are important to simulations in the high-energy, high-density physics regime, e.g., for inertial confinement fusion and astrophysics. Moment-based hybrid Monte Carlo (MC) methods have demonstrated great potential for accelerated solutions to TRT problems [1, 2, 3]. These nonlinear acceleration methods iterate between a high-order (HO) transport equation and a low-order (LO) system formulated with angular moments and a fixed spatial mesh. Physics operators that are too expensive for the HO solver to resolve directly, e.g., photon absorption and emission, are moved to the LO system. The lower-rank LO equations can be solved with Newton methods to allow for non-linearities in the LO equations to be efficiently resolved. The high-order (HO) problem is defined by the radiation transport equation with sources computed with the previous LO solution. A MC transport solution to the HO problem is used to construct consistency terms that appear in the LO equations. These consistency terms preserve the accuracy of the HO solution in the next LO solve.

Previously, residual Monte Carlo (RMC) methods have been used to provide efficient solution to the HO transport problem [1, 2]; high-fidelity solutions, with minimal statistical noise, have been achieved for problems with optically-thick, diffusive regions that lead to slowly varying solutions. However, the results in these works used a backward Euler (BE) discretization for the time variable, which can inaccurately disperse radiation wavefronts in optically thin problems. We have extended the work in [2] to include higher-accuracy MC treatment of the time variable for the radiation unknowns. The exponentially-convergent Monte Carlo (ECMC) algorithm was modified to include integration of the time variable; this includes the introduction of a step, doubly-discontinuous (SDD) trial space representation in time. A new parametric closure of the LO equations, introducing additional time-closure consistency terms, was derived to capture the time accuracy of the HO ECMC simulations. The LO equations can preserve the accuracy of MC radiation transport treatment in time, with the same numerical expense as Backward Euler (BE) time-discretized S_2 equations. Herein we briefly describe the algorithm, and we present results for one-dimensional (1D), grey test problems. We compare our method to the implicit MC (IMC) method [4], the standard MC solution method for TRT problems.

ACKNOWLEDGMENTS

METHODOLOGY

The 1D, grey TRT equations consist of the radiation and material energy balance equations, i.e.,

$$\frac{1}{c}\frac{\partial I(x,\mu,t)}{\partial t} + \mu\frac{\partial I(x,\mu,t)}{\partial x} + \sigma_a I(x,\mu,t) = \frac{1}{2}\sigma_a ac T^4(x,t) \tag{1}$$

$$\rho c_v \frac{\partial T(x,t)}{\partial t} = \sigma_a \phi(x,t) - \sigma_a ac T^4(x,t), \tag{2}$$

where physical scattering could optionally be included in Eq. (1), and appropriate initial and boundary conditions are specified. In the above equations x is the position, t is the time, μ is the x-direction cosine of the angular intensity $I(x,\mu,t)$, σ_a is the macroscopic absorption cross section (cm^{-1}), and a, c, ρ, and c_v are the radiation constant, speed of light, mass density, and specific heat, respectively. The desired transient unknowns are the material temperature $T(x,t)$ and the mean radiation intensity $\phi(x,t) = \int_{-1}^{1} I(x,\mu,t)\mathrm{d}\mu$. The mean intensity is related to the radiation energy density E_r by the relation $E_r = \phi/c$. The equations can be strongly coupled through the gray Planckian emission source $\sigma_a ac T^4$, which is a nonlinear function of temperature, and the absorption term $\sigma_a\phi$.

In our HOLO algorithm, the LO solver resolves the material temperature spatial distribution $T(x)$ over each time step, whereas the HO solver computes weighted angular and temporal averages of $I(x,\mu,t)$. The fully-discrete LO equations are based on space-time-angle moments of the TRT equations, formed over a spatial finite-element (FE) mesh. Angularly, the LO radiation equations are similar to S_2 equations, with element-averaged consistency parameters that are weighted averages of μ. The BE time discretization is applied to emission source throughout, but the radiation variables are left in terms of time-averaged and end-of-time-step unknowns. This is analagous to the time integration in IMC [4]. Additional consistency parameters are introduced in parametric closures that eliminate the auxillary time-unknowns from the LO radiation equations. If the angular and time consistency parameters were estimated exactly, then the LO equations would exactly preserve HO moments, neglecting spatial discretization error. The HO consistency parameters are lagged in each LO solve. The LO equations always conserve energy, independent of the accuracy of the consistency terms.

The solution to the LO system is used to construct a spatially linear-discontinuous (LD) FE representation of the emission source on the right hand side of Eq. (1). This defines a fixed-source, pure absorber transport problem for the HO operator. This HO transport problem is solved with the ECMC algorithm. The ECMC algorithm is an iterative RMC method that uses batches of MC histories to estimate the error in the current trial-space estimate of $I(x,\mu,t)$. It is noted that because we are not using mesh adaptation in this work, exponential

convergence in iterations cannot be maintained, but reduced variance from the RMC formulation can still be achieved. The output from ECMC is a projection $\tilde{I}(x, \mu, t)$ of the intensity onto the chosen trial space. Once computed, $\tilde{I}(x, \mu)$ is used to directly evaluate the necessary LO angular and time-closure consistency parameters.

Iterations between the HO and LO solves can increase accuracy in strongly nonlinear problems. However, for the problems tested here, only a single HO solve is performed during each time step. Thus, the HOLO algorithm, for the n'th time step, is

1. Perform a LO solve to produce an initial guess for $T_{LO}^{n+1}(x)$ and $\phi_{LO}^{n+1}(x)$, based on consistency terms estimated with $\tilde{I}^n(x, \mu)$ and a BE time discretization.

2. Solve the HO system for $\tilde{I}_{HO}(x, \mu, t)$ using ECMC, based on the current LO estimate of the emission source.

3. Compute LO angular and time-closure consistency parameters with $\tilde{I}_{HO}(x, \mu, t)$.

4. Solve the LO system using HO consistency parameters to produce a new estimate of ϕ_{LO}^{n+1} and T_{LO}^{n+1}.

5. Store $\tilde{I}^{n+1}(x, \mu) \to \tilde{I}^n(x, \mu)$, and move to the next time step.

The LO System

To derive the LO equations, we reduce the dimensionality of Eq. (1) and Eq. (2) by taking spatial, angular, and temporal integrals. The spatial moments are taken over each spatial cell i: $x \in [x_{i-1/2}, x_{i+1/2}]$, weighted with the standard linear Lagrange interpolatory FE basis functions. For example, the left moment operator is defined by

$$\langle \cdot \rangle_{L,i} = \frac{2}{h_i} \int_{x_{i-1/2}}^{x_{i+1/2}} b_{L,i}(x)(\cdot)\mathrm{d}x, \qquad (3)$$

where $h_i = x_{i+1/2} - x_{i-1/2}$ is the width of the spatial element and $b_{L,i}(x) = (x_{i+1/2} - x)/h_i$ is the basis function corresponding to position $x_{i-1/2}$. Angularly, the equations are integrated over the positive and negative half ranges. The angular integrals of the intensity are defined as $\phi^{\pm}(x) = \pm 2\pi \int_0^{\pm 1} I(x, \mu)\mathrm{d}\mu$. Finally, the equations are integrated over the n'th time step for $t \in [t^n, t^{n+1}]$ with width $\Delta t = t^{n+1} - t^n$.

The $\langle \cdot \rangle_{L,i}$ moment, positive half-range integral, and integration over a time step of Eq. (1) yields

$$\frac{\langle \phi \rangle_{L,i}^{+,n+1} - \langle \phi \rangle_{L,i}^{+,n}}{c \Delta t} - 2\overline{\mu}_{i-1/2}^+ \overline{\phi}_{i-1/2}^+ + \{\overline{\mu}\}_{L,i}^+ \langle \overline{\phi} \rangle_{L,i}^+ + \{\overline{\mu}\}_{R,i}^+ \langle \overline{\phi} \rangle_{R,i}^+$$
$$+ \sigma_{a,i}^{n+1} h_i \langle \overline{\phi} \rangle_{L,i}^+ = \frac{h_i}{2} \langle \sigma_a^{n+1} ac T^{n+1,4} \rangle_{L,i}, \quad (4)$$

where overlined quantities denote time averaging. The time-averaged angular consistency terms are approximated with previous HO solution, e.g.,

$$\overline{\{\mu\}}_{L,i}^+ = \frac{\dfrac{2}{h_i} \int\limits_0^1 \int\limits_{x_{i-1/2}}^{x_{i+1/2}} \mu\, b_{L,i}(x)\overline{I}_{HO}(x, \mu)\mathrm{d}x\mathrm{d}\mu}{\dfrac{2}{h_i} \int\limits_0^1 \int\limits_{x_{i-1/2}}^{x_{i+1/2}} b_{L,i}(x)\overline{I}_{HO}(x, \mu)\mathrm{d}x\mathrm{d}\mu}. \qquad (5)$$

where $\overline{I}(x, \mu)$ is a time-averaged LDFE projection in x and μ, as explained in the next section. For simplicity, the face terms are eliminated from the system using a lumped LDFE spatial approximation, with upwinding [2]. There is some inconsistency introduced in this approximation, but it has proven stable for problems tested and demonstrates preservation of the equilibrium diffusion limit.

Each LO equation must be closed in time consistently with the HO equations. Previous work has enforced consistency in time by adding a local artificial source to the time-discretized LO equations in each cell to cancel inconsistencies [3]. We will alternatively use a local, parametric closure for the radiation unknowns. Quantities at t^n are known from the previous time step or an initial condition. Thus, Eq. (4) can be written exclusively in terms of time-averaged radiation unknowns, if $\langle \phi \rangle_{L,i}^{n+1}$ is eliminated from the system. The simplest closure is a weighted average

$$\langle \phi \rangle_{L,i}^{+,n+1} \approx \gamma_{L,i,HO}^+ \langle \overline{\phi} \rangle_{L,i}^+ \qquad (6)$$

where $\gamma_{L,i,HO}^+$ is a time-closure consistency parameter. The consistency parameter can be determined from Eq. (6) using moments of $\overline{I}_{HO}(x, \mu)$ and $I_{HO}^{n+1}(x, \mu)$. For the initial LO solve, within a time step, the angular parameters are calculated based on the $\tilde{I}_{HO}^n(x, \mu)$ and all γ values are set to unity, producing a BE discretization. Other closures, e.g., a modified Crank-Nicolson, have been explored. In optically thin problems, the problem is nearly linear, and the choice of this closure has minimal effect on results because all other auxilary unknowns have been eliminated from the system with HO information. Once time-averaged unknowns have been calculated, the local time closures provide the $\phi_{LO}^{n+1}(x)$. There are four time-closure consistency parameters, for each LO element.

The other radiation and material energy equations can be derived analogously. More specifics on the angular and spatial manipulation of equations can be found in [2]. Summing the equations over all cells, a global, nonlinear LO system of equations for the moment unknowns is defined. This system of equations is solved using a Newton-Picard method, as in previous work [2].

The Residual MC High Order Solver

To apply the ECMC algorithm, it is necessary to have a trial space representation of the solution for all phase space variables. The intensity is represented in x and μ with a LDFE projection [2]. This projection, over each space-angle cell, is linear and preserves the zeroth, and first moment in x and μ. A step, doubly-discontinuous (SDD) trial space is used to represent the intensity as a function of t. The trial space representation for $I(x, \mu, t)$ becomes

$$\tilde{I}(x, \mu, t) = \begin{cases} \tilde{I}^n(x, \mu) & t = t^n \\ \overline{I}(x, \mu) & t^n < t < t^{n+1} \\ \tilde{I}^{n+1}(x, \mu) & t = t^{n+1} \end{cases} \qquad (7)$$

where we have used $\overline{I}$ to denote the time-averaged LDFE projection in x and μ of the intensity over the interior of the time step; the LDFE projections at t^n and t^{n+1} are denoted

$\tilde{I}^n$ and $\tilde{I}^{n+1}$, respectively. The SDD trial space provides a projection for all the desired unknowns that result from time-integration of the transport equation. Another benefit of this trial space is it allows for the residual sampling infrastructure from the time-discrete formulation to be used.

The transport equation to be solved by ECMC is given by Eq. (1), but with a known LDFE Planckian emission source:

$$\mathbf{L}I(x,\mu,t) = q_{LO}(x) \qquad (8)$$

where q_{LO} denotes the latest estimate of the isotropic emission source, computed with $T_{LO}^{n+1}(x)$, and is constant for the entire HO solve. The *continuous* linear operator $\mathbf{L}$ includes the streaming, removal, and time derivative on the left-hand side of Eq. (1). The m'th approximate solution to Eq. (8) is $\tilde{I}^{(m)}$, where m identifies the MC batch. The m'th residual is $r^{(m)} = q - \mathbf{L}\tilde{I}^{(m)}$, which with manipulation gives the error equation

$$\mathbf{L}(I - \tilde{I}^{(m)}) = \mathbf{L}\epsilon^{(m)} = r^{(m)}, \qquad (9)$$

where I is the exact solution (for the HO problem which has discretization error from $\tilde{I}^n(x,\mu)$ and q_{LO}) and $\epsilon^{(m)}$ is the error in $\tilde{I}^{(m)}$. The operator $\mathbf{L}$ in Eq. (9) is inverted without discretization via MC simulation, and then projected, to produce a LDFE projection of the error in $\tilde{I}^{(m)}$, i.e., $\tilde{\epsilon}^{(m)} = \mathbf{L}^{-1}r^{(m)}$. The MC simulation samples particles from the source $r^{(m)}$, which produces negative and positive weights. Histories are tracked in space, angle, and time, as for IMC [4]. The LDFE projections of the error $\bar{\epsilon}$ and ϵ^{n+1} are computed using generalizations of volumetric path-length and particle density estimators. The estimators are weighted by appropriate basis functions, over each space-angle cell, and account for particles streaming without interaction [2]. The discontinuities in Eq. (7) introduce δ-function sources at t^n and t^{n+1} because of the time derivatives. However, the contribution from the discontinuity source at t^{n+1} can be analytically determined and is not sampled.

The ECMC algorithm is

1. Initialize $\tilde{I}^{(0)}(x,\mu,t)$ with $\tilde{I}^n(x,\mu)$.

2. Compute $r^{(m)}$.

3. Estimate $\tilde{\epsilon}^{(m)} = \mathbf{L}^{-1}r^{(m)}$ with N Monte Carlo histories.

4. Compute $\tilde{I}^{(m+1)} = \tilde{I}^{(m)} + \tilde{\epsilon}^{(m)}$

5. Optionally repeat $2-4$ for desired number of batches.

A drawback of this algorithm is that a truncation error occurs by keeping only the LDFE projection of the intensity between time steps. Adaptive mesh refinement is likely necessary to efficiently capture rapidly-varying solutions, but this could be included in the iterative ECMC algorithm.

RESULTS AND ANALYSIS

We have simulated two 1D, grey test problems to demonstrate the efficacy of our HOLO algorithm: an optically thin problem and a standard Marshak wave test problem. Solutions are compared to results from an IMC code [5]. A normalized, spatially integrated measure of variance in cell-averaged

radiation energy densities $E_{r,i}^{n+1}$ was computed, based on the solution at the end time. The variance metric is

$$\|s\| = \left(\sum_{i=1}^{N_c} \hat{S}_i^2 \Big/ \sum_{i=1}^{N_c} \left(\hat{E}_{r,i}^{n+1} \right)^2 \right)^{1/2}, \qquad (10)$$

where N_c is the number of spatial cells and $\hat{S}_i^2$ and $\hat{E}_{r,i}^{n+1}$ are the sample variance and mean of $E_{r,i}^{n+1}$, as estimated from 20 independent simulations. A figure of merit (FOM) is then defined as $\text{FOM} = \left(N_{\text{tot}} \|s\|^2 \right)^{-1}$, where N_{tot} is the total number of histories performed for that problem setup. All FOM results are relative for a particular problem and normalized to a particular IMC simulation. All results for the HOLO method depict the LO result.

Optically Thin Problem

For this problem, material properties are uniform throughout a 2.0 cm wide domain with $\rho c_v = 0.01374$ GJ cm^{-3} keV^{-1}, $a = 0.01372$ GJ cm^{-3} keV^4, and $\sigma_a = 0.2$ cm^{-1}. The material and radiation are initially in equilibrium at an effective temperature of 0.01 keV. An isotropic incident intensity with $T_r = 0.150$ keV is applied at $x = 0$ for $t > 0$; the incident intensity on the right boundary is 0.01 keV. Solutions are depicted as an effective radiation temperature $T_r = (\phi/(ac))^{0.25}$. The values for T_r^{n+1} from the last time step are compared for IMC, the HOLO method with continuous time treatment (HOLO-TC), and the HOLO method with full BE time discretization (HOLO-BE) in Fig. 1; the simulation end time is 0.003 sh (1 sh=10^{-8} s). The HOLO-TC and HOLO-BE results were generated with 30 uniform μ cells, and all spatial meshes used 200 cells. At smaller time step sizes, the effects of projecting the solution between time steps become apparent in the HOLO-TC results, leading to visible inaccuracies. For $\Delta t = 0.005$ sh, there is good agreement between the HOLO-TC results and IMC. The HOLO-BE results do not accurately capture the wavefront location, as expected. IMC demonstrates noise in the equilibrium regions of the problem. The dispersion near the foot of the wave is caused by the lumped LDFE approximation in the LO equations as compared to the HO LDFE projection, but this discrepancy is minimal in terms of E_r^{n+1} rather than T_r^{n+1}.

Table. I compares FOM values for E_r^{n+1}, for two different Δt values. HOLO results were generated for the case of 1 and 2 uniform batches, with the same total number of histories per time step. At low particle counts for the larger time step size, the HOLO-TC method demonstrates substantial noise, leading to instabilities. This is due to $\tilde{I}^{n+1}(x,\mu)$ being poorly estimated. For the 2 batch case, the estimate from the first batch leads to less error in $\tilde{I}^{n+1}(x,\mu)$ in the second batch. At smaller time-steps there is an increase in statistical efficiency, however the accuracy is reduced due to an increase in projection error. A finer mesh size is needed to produce higher accuracy.
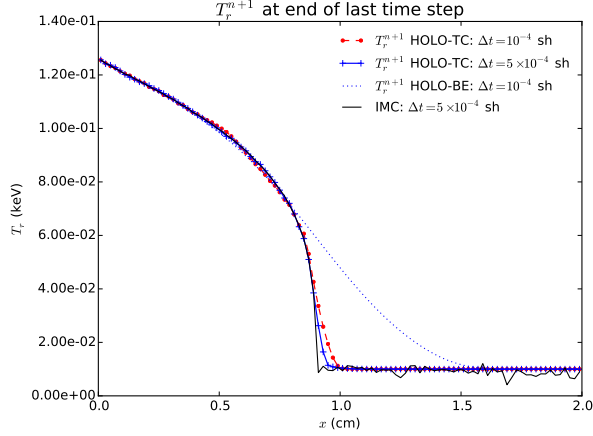
Fig. 1. Comparison of radiation temperatures for optically thin problem.

TABLE I. Comparison of FOM for the optically thin problem. Simulation end time is $t = 0.003$ sh. The numbers in parenthesis indicate number of batches per time step.

	FOM		
	$\Delta t = 5 \times 10^{-4}$ sh		
hists./step	IMC	HOLO-TC(1)	HOLO-TC(2)
30,000	1.00	0.03	0.31
300,000	0.93	1.38	1.65
1,000,000	1.10	3.42	2.00
	$\Delta t = 10^{-4}$ sh		
hists./step	IMC	HOLO-TC(1)	HOLO-TC(2)
30,000	1.00	42.00	6.95
300,000	0.98	94.47	12.38

TABLE II. Comparison of FOM for the Marshak wave problem. Simulation end time is **t = 3.0** sh.

	FOM		
hists./step	IMC	HOLO-TC (2)	HOLO-BE (2)
300,000	1.00	0.43	2050
1,000,000	0.94	15.95	1806

Marshak Wave Problem

This problem has the same material properties as the optically thin problem except $\sigma_a(T) = 0.001T^{-3}$, and the initial temperature is 2.5×10^{-5} keV. The time step size is linearly increased from 0.001 sh to a maximum step of 0.01 sh over the first 10 time steps. It was found for this problem that it was necessary to use more than one batch for the HOLO-TC algorithm to stably converge. This is because few particles reach t^{n+1} in optically thick regions.

Although not shown, for 10^6 histories and 200 mesh cells, there was good agreement between the HOLO-BE, HOLO-TC, and IMC methods; this slowly-evolving problem can be accurately modeled with the BE time discretization, but the MC time closure demonstrates stability in the mix of optically thick and thin regions that occurs as the material heats. Table II

compares FOM values for IMC and the HOLO method with MC time treatment and for a BE discretization. The HOLO-TC is not as statistically efficient as HOLO-BE for this problem, but is more efficient than IMC with sufficient histories.

CONCLUSIONS

Initial results demonstrate that RMC methods can be extended to include the time variable, increasing accuracy in optically thin regions compared to a BE discretization. Our ECMC algorithm can be more statistically efficient than IMC, with sufficient batch sizes, although sufficient mesh resolution is needed to limit projection error between time steps. We have demonstrated a new approach to closing the LO equations in time that produces accurate solutions. Long-term, an ideal solution would require no projection between time steps, which will likely require an operator split on the radiation time derivative. At this point, we believe that the SDD trial space in time suffers from inaccuracy because only histories that reach the end-of-time step contribute to I^{n+1} and because of the flat interior representation. Alternatively, the LDFE trial space could include the time variable. Then, all particle tracks contribute to slopes over the interior of the time step. However, there is some additional truncation error as $\tilde{I}^{n+1}$ is an extrapolated quantity. This trial space requires substantial modifications to the residual sampling algorithm because of how the residual is currently sampled. An importance sampling methodology has been developed but remains to be implemented. Modifications to the sampling algorithm are necessary to extend to higher spatial dimensions, so determining if our approach is efficient will be beneficial to future work. We will include results for the LDFE time representation for the full paper.

REFERENCES

1. J. WILLERT and H. PARK, "Residual Monte Carlo High-order Solver for Moment-Based Accelerated Thermal Radiative Transfer Equations," *Journal of Computational Physics*, **276**, 405 – 421 (2014).
2. S. BOLDING, M. CLEVELAND, and J. MOREL, "A High-Order Low-Order Algorithm with Exponentially-Convergent Monte Carlo for Thermal Radiative Transfer," *Nuclear Science & Engineering: M&C 2015 Special Issue* (Jan. 2017), forthcoming.
3. A. B. WOLLABER, H. PARK, R. LOWRIE, R. RAUEN-ZAHN, and M. CLEVELAND, "Radiation Hydrodynamics with a High-Order, Low-Order Method," in "ANS Topical Meeting, International Topical Meeting on Mathematics and Computation," Nashville Tennessee (2015).
4. J. A. FLECK, JR. and J. D. CUMMINGS, JR., "An Implicit Monte Carlo Scheme for Calculating Time and Frequency Dependent Nonlinear Radiation Transport," *J. Comput. Phys.*, **8**, *3*, 313–342 (Dec. 1971).
5. T. URBATSCH ET AL., "Milagro Version 2 An Implicit Monte Carlo Code for Thermal Radiative Transfer: Capabilities, Development, and Usage," (2006), los Alamos National Laboratory Report LA-14195-MS.